Martin Walenta, BSc

Improving NMR measurements by utilizing deuterium isotopic effects, inlays and cyclodextrins

MASTER'S THESIS

to achieve the university degree of

Master of Science

Master's degree programme: Chemistry

submitted to

Graz University of Technology

Supervisor

Ao.Univ.-Prof. Mag. Dr.rer.nat. Klaus Zangger

Institut für Chemie

Graz, March 2019

AFFIDAVIT

I declare that I have authored this thesis independently, that I have not used other than the declared sources/resources, and that I have explicitly indicated all material which has been quoted either literally or by content from the sources used. The text document uploaded to TUGRAZonline is identical to the present master‘s thesis.

Date

Signature

Acknowledgements

I would like to thank my supervisor Dr. Klaus Zangger for his friendly guidance into the world of NMR and all the patience and time he has given to me. Moreover I would like to thank him for all the opportunities to go on diverse trips with the working group and for the opportunity to give a poster presentation at the "Adriatic NMR" in Croatia.

I would like to thank all the members of the working group for the pleasant and relaxed working atmosphere and for all the encouraging and helpful discussions and comments.

I especially would like to thank Ing. Bernd Werner for always helping me out with problems at the NMR and having an open ear for me. I also really appreciated it to always have someone to go with for lunch and also to tattle about everything.

Furthermore I appreciated the productive and helpful collaboration with Alexander Swoboda, BSc, who helped me out with my synthetic experiments.

I would like to thank Dr. Olaf Kunert for providing his rutin data and giving me input for further experiments.

I also would like to say thank you to my family, friends and everyone that helped me to relax and supported me throughout the whole time. It really was a pleasant time.

TABLE OF CONTENTS

ABBREVIATIONS

ABS	acrylonitrile butadiene styrene
DIS	differential isotope shift
DMF	dimethylformamide
DMSO	dimethyl sulfoxide
equiv.	equivalent
EtOH	ethanol
FID	free induction decay
h	hour
MDA	mandelic acid
min	minute
MON	mandelonitrile
NMR	nuclear magnetic resonance
PED	1-phenyl-1,2-ethanediol
PL	2-pantolactone
ppm	parts per million
SLA	stereolithography
SNR	signal to noise ratio
THF	tetrahydrofuran
TXI	triple resonance inverse

1. INTRODUCTION

NMR spectroscopy is arguably the most often used technique for the structure elucidation of small organic, inorganic and biomolecules. Therefore, it is very important to improve the sensitivity, resolution and information content of NMR experiments.[1,2] That's why we thought of three methods that could be used to improve NMR measurements.

The first improvement concerns the distinction of protonated heteroatom groups from unprotonated ones. For this we want to make use of the so called "Deuterium Isotope Effect" defined by Pfeffer et al..[3] With this effect, it should be possible to cause a shift in carbon atoms, which are next to protonated heteroatoms.

In the second improvement, we wanted to optimize the signal-to-noise ratio of measurements by designing an inlay that optimizes the magnetic field homogeneity in an NMR-tube. The idea came from the fact that there are special NMR-tubes (Shigemi©) that can already do this, but are correspondingly expensive and made out of a special glass.[4] We would like to see whether this is also possible with a rather cheap 3D-print.

The last improvement is a side project to test whether cyclodextrins can be substituted on a single hydroxy group with little effort and our available laboratory equipment and whether this can be used for enantiomeric resolution. If possible, one wanted to find a derivative that could be used as an universal addition to NMR experiments in order to determine chiral purities of molecules, as it has already been shown for isolated cases.[5,6]

2. DETERMINATION OF HETEROATOM PROTONATION STATES

2.1. Theoretical

During the NMR assignment, carbon-bound heteroatoms (oxygen, nitrogen, sulfur) which can potentially bind exchangeable protons cause problems when the protonation state cannot be unambiguously determined. So, for example it is often difficult to differentiate if a carbon-bound oxygen belongs to an ether or rather an alcohol group, unless the alcoholic OH is visible in the proton spectrum and multi-bond correlations to a carbon nucleus can be found. Often such correlations cannot be found due to exchange broadening of the proton attached to the heteronucleus or small scalar coupling across the heteroatom.

2.1.1. Use of the Isotopic effect

It has been known since the early days of solution NMR spectroscopy that the substitution of hydrogen against deuterium can used to obtain structural information. Upon exchange of hydrogen with deuterium, the dynamic state of a molecule changes and therefore the electronical structure is modified, which leads to an alteration of the magnetic shielding of various nuclei in the vicinity.[7,8] Early reports also showed that deuterium isotope shifts of exchangeable protons on directly attached carbon nuclei can be used to identify functional groups in peptides[9,10], sugars[3,11] and other substances.[12–14] These experiments are usually done with completely deuterated species[9] or special dual cell NMR-tubes[3,11,14] to see the exchanging groups as a duplet and are mostly measured in H_2O/D_2O[3,10,11,14] or DMSO.[12,13] Here we show that heteroatoms (oxygen, nitrogen and sulfur) with directly attached hydrogens (alcohols, primary or secondary amines and thiols) can be differentiated from those without directly bound protons (ethers, tertiary amines and thioethers) by the differential isotope shifts in a variety of organic solvents for basically any kind of molecules. A few percent of H_2O or D_2O have to be added to the preferred solvent to achieve complete equilibrium of all exchangeable protons. The organic solvent does not need to be miscible with water.

2.1.2. DIS values

The ^{13}C chemical shift difference induced by a replacement of the exchangeable proton to deuterium was defined as differential isotope shift (DIS). DIS was selected to be the difference of the chemical shifts in parts per million (ppm) between the ^{13}C shift observed in the solvent with H_2O added and the upfield shift in the presence of D_2O ($\delta^{13}C_{H_2O}$-$\delta^{13}C_{D_2O}$).[3] In each class of compounds, a variety of compounds was tested in order to examine the range of validity of DIS measurements in various organic solvents.

2.1.2.1. Alcohols and ethers

Differential isotope shifts of various alcohols and ether and other oxygen containing groups in methanol are shown in the following Figures. An alcoholic group leads to a DIS of 0.09 ± 0.02 ppm for the carbon to which it is attached. (Figure 2-1)

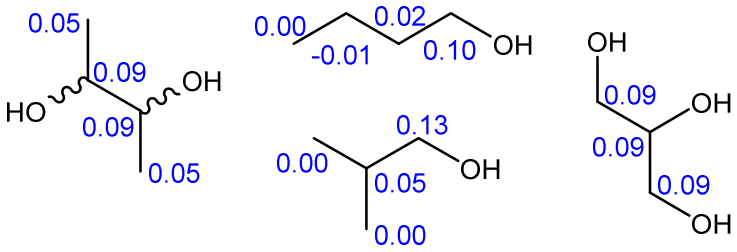

Figure 2-1 Various alcohols and the corresponding DIS values in methanol [ppm].

Whereas an ether group leads to a DIS of 0.00 ± 0.01 ppm for the corresponding α-carbon. (Figure 2-2)

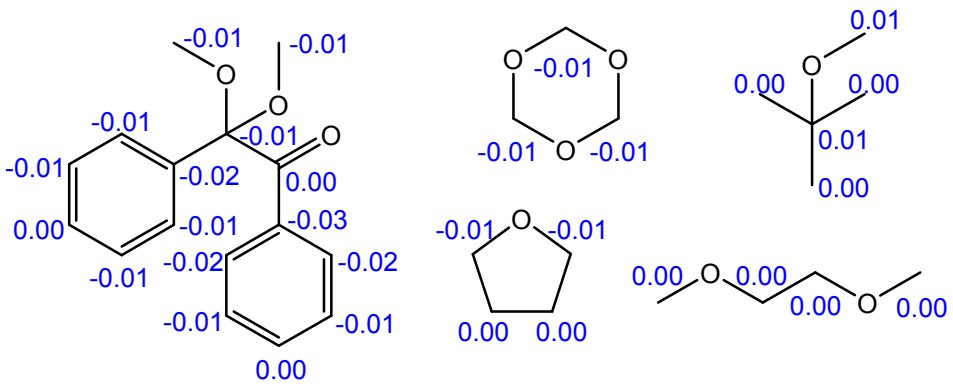

Figure 2-2 Various ethers and the corresponding DIS values in methanol [ppm].

Moreover, in compounds where both hydroxyl and ether groups are present, there is a clear upfield shift of the $\alpha^{13}C$-atom of alcoholic groups. Sometimes a field shift can be observed

for neighboring ^{13}C-atoms. However, the field shift is rather weak and does not seem to follow a simple pattern. (Figure 2-3)

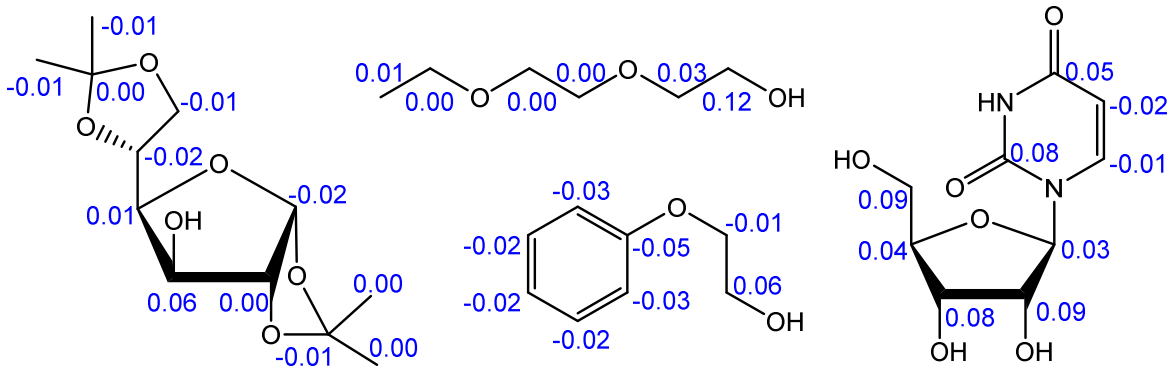

Figure 2-3 Chemicals containing a least one hydroxyl and one ether group. The corresponding DIS values measured in methanol are given in [ppm].

DIS values were also evaluated for several other functional groups carrying no exchangeable protons to validate the approach for the identification of exchangeable protons (Figure 2-4).

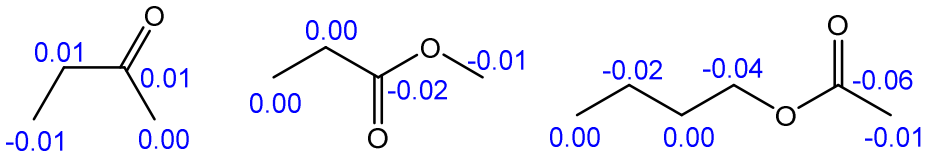

Figure 2-4 Chemicals containing alternate functional groups and the corresponding DIS values in methanol [ppm].

In order to compare the measurement in the different solvents, the mean and the standard deviation of the α-carbons shift from the chemicals in Figure 2-1 and Figure 2-3 were calculated.

Table 1 Comparison of the alcohols from Figure 2-1 and the mixtures of Figure 2-3 in different solvents. (DIS in [ppm])

	methanol	pyridin	$CDCl_3$
alcohols	0.10 ± 0.02	0.12 ± 0.01	0.15 ± 0.02
mixtures	0.08 ± 0.02	0.11 ± 0.01	0.12 ± 0.02
combination	0.09 ± 0.02	0.11 ± 0.01	0.14 ± 0.02

From this data, it can be seen that such measurements are useful for distinguishing alcohols from ethers in all solvents tested. The DIS values are comparable, although slightly lower in methanol.

2.1.2.2. Amines

In parallel with alcohols and ethers, various primary, secondary and tertiary amines were selected and measured in methanol, pyridine and chloroform. The observed DIS values for both the α- and β-position are similar to alcohols for primary and secondary amines and rather small, similar to ethers for tertiary amines. Again we see upfield shifts for the α-carbons.

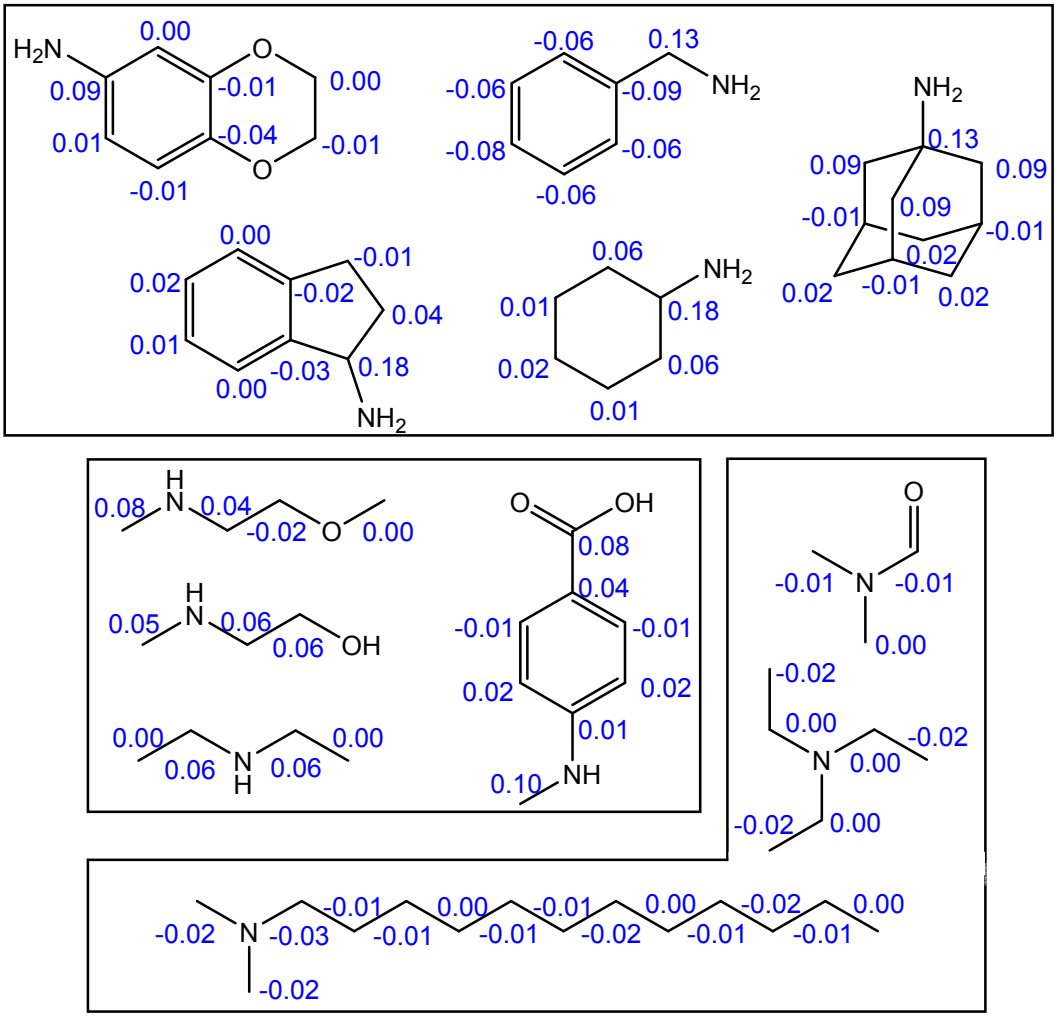

Figure 2-5 Various primary, secondary and tertiary amines and the corresponding DIS values in methanol [ppm].

The differentiation between primary and secondary amines through their DIS values is not unambiguous. However in most cases investigated primary and secondary amines show DIS values on the α-carbon of 0.14 ± 0.04 ppm and 0.07 ± 0.02 ppm, respectively.

It is also interesting how the aromatic ^{13}C-atoms of benzylamine are affected by deuterium exchange. A downfield shift occurs in all ^{13}C-atoms except the α position. This shows that the shielding of the benzyl system is heavily influenced just by exchanging the hydrogen with a deuterium.

To compare the primary and secondary amines in the different solvents the mean and standard deviation of the α-carbons shift were calculated.

Table 2 Comparison of the prim. amines from and the sec. amines of Figure 2-5 in different solvents. (DIS in [ppm])

	methanol	pyridin	$CDCl_3$
prim.	0.14 ± 0.04	0.18 ± 0.03	0.17 ± 0.05
sec.	0.07 ± 0.02	0.10 ± 0.01	0.10 ± 0.05

As for alcohols, the DIS values in methanol are somewhat smaller than in chloroform and pyridine.

2.1.2.3. Thiols and thioethers

Additionally various sulfur containing chemicals were selected and measured in methanol, pyridine and chloroform. Again a upfield shift for the α-carbons can be observed.

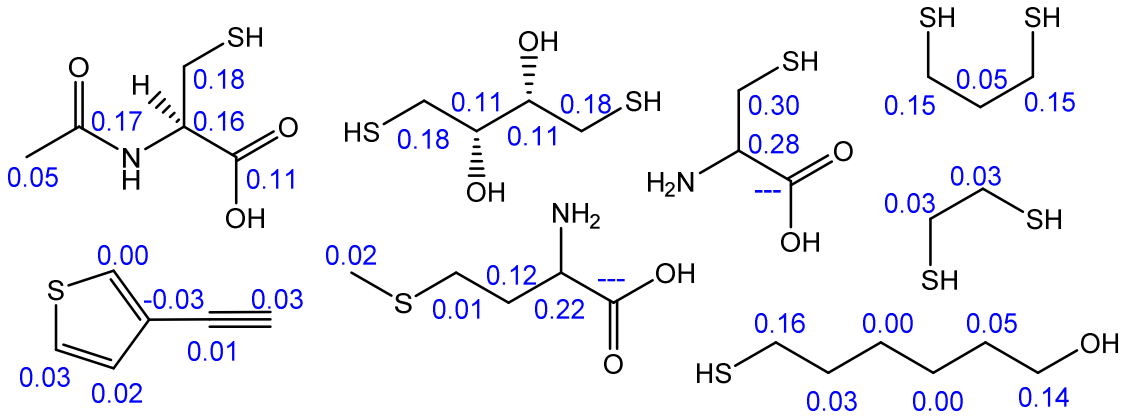

Figure 2-6 Various sulfur containing chemicals and their measured shifts in methanol are given in DIS [ppm]. --- shows, that for that specific ^{13}C-atom no peak could be found in the NMR. This resulted of the fact that the signal for quaternary carbon atoms are rather weak in comparison and that the solubility in methanol was rather low.

For a protonated group 1,2-ethandithiol shows a rather weak shift in methanol, a rather big one of 0.37 ppm in pyridine and an approximately expected shift of 0.15 ppm in chloroform. For this reason it was left out for the calculations of the average DIS values.

Table 3 Comparison of the thiol-groups from Figure 2-6 in different solvents. (DIS in [ppm])

	methanol	pyridin	$CDCl_3$
thiols	0.19 ± 0.06	0.14 ± 0.02	0.16 ± 0.07

The rather high standard deviation results from the unexpected high upfield shift in L-cysteine. This does not happen in pyridin, since L-cysteine was insoluble in this solvent.

2.1.2.4. Erythromycin

With the help of erythromycin we now want to show how well this method works in a practical example. Erythromycin is suitable for this because it has a total of five hydroxyl, five ether, a tertiary amine, an ester and a carbonyl group. Furthermore the values for the various ether and hydroxyl groups are relatively close together, which makes the correct assignment even more difficult. The carbonyl group was not measured in the ^{13}C-spectrum because it was above the spectrum limit of 220 ppm and was not further investigated since it is not relevant to this experiment. The assignment of the ^{13}C-atoms is done by comparing it with a previously obtained assignment, which we got from a cooperation with Prof. Predrag Novak, and the help of our methodology. To check the accuracy, an HMBC measurement was taken and compared with the assignment. The DIS values of the various carbons were assigned as shown in Figure 2-7.

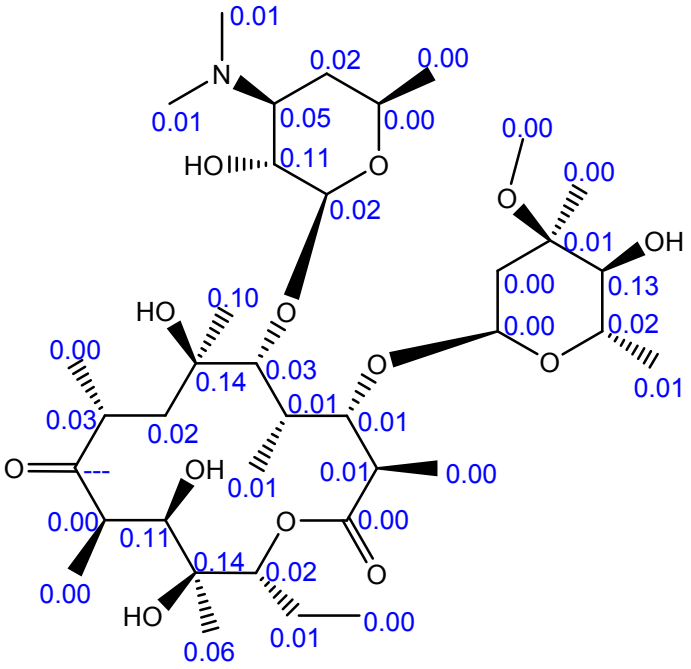

Figure 2-7 Chemical structure of erythromycin. DIS values measured in methanol are given in ppm upfield shift. The signal for the carbonyl group was outside of the spectrum limit of 220 ppm and was therefore given as ---.

It can be seen that all ^{13}C-atoms adjacent to a hydroxyl group have a DIS value above 0.10 ppm. Incidentally it can be seen that methyl groups which are bonded to the same quaternary carbon as a hydroxyl group also have an increased DIS value. This could also be used to assign their peaks more easily.

2.1.2.5. Rutin

Another good example is rutin with six aliphatic and four aromatic hydroxyl groups as well as five ethers. In the ^{13}C-spetrum we get nine peaks in the area between 68 and 78 ppm which all belong to α^{13}C-atoms of either an aliphatic OH or an ether group. To correctly assign these peaks without time-consuming 2D experiments or even differentiate which peak belongs to an ether or a hydroxyl group seems rather impossible. But with the help of DIS values it is far simpler to see which α^{13}C-atom belongs to each functional group which eases the further assignment process. (Figure 2-8)

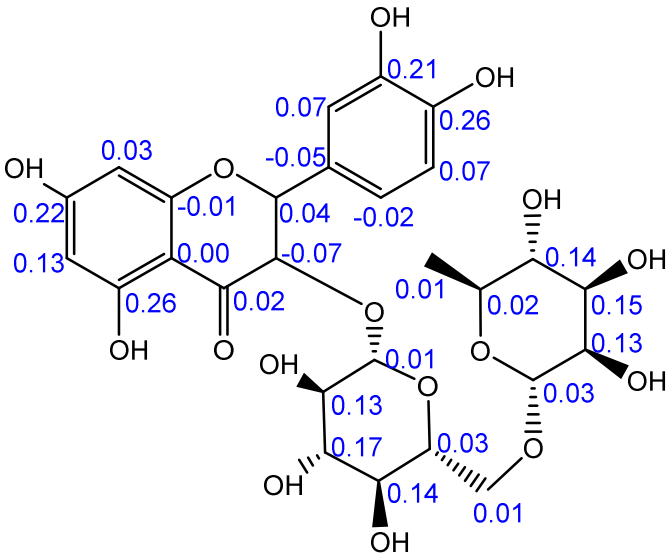

Figure 2-8 Chemical structure of rutin. DIS values measured in methanol, like usually (10% v/v H_2O/D_2O), are given in ppm upfield shift.

The aromatic hydroxyl groups are comparatively easy to assign, because of the well studied benzylic system. Nevertheless, being able to assign the hydroxyl-groups by simply looking at the DIS values without calculating the approximate shift of each aromatic atom is convenient. To test out if this kind of method is also possible with less water inside the sample another measurement was taken.

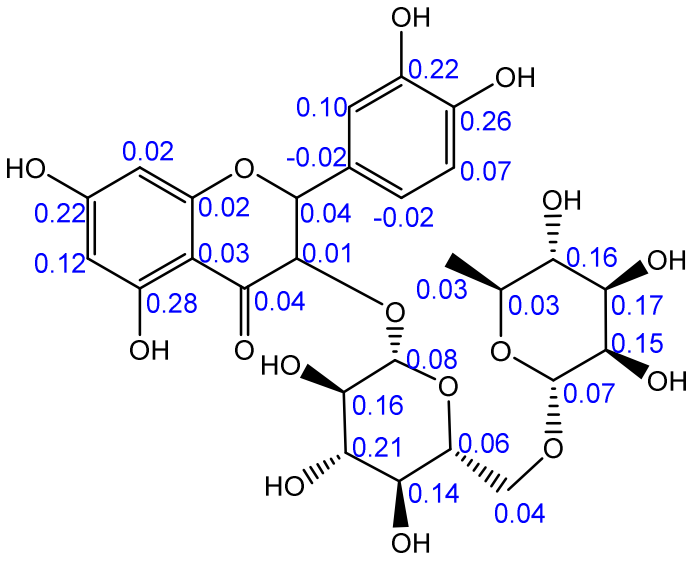

Figure 2-9 Chemical structure of rutin. DIS values this time measured in methanol (2% v/v H_2O/D_2O) are given in ppm upfield shift.

As can be seen by comparing the results from Figure 2-8 and Figure 2-9, it also works with only 2% v/v water inside the sample. The DIS values of each carbon atom stays approximately the same and the easier assignment is still possible.

2.2. Experimental

All chemicals were purchased from Sigma-Aldrich (St. Louis, MO, USA) at >98% purity and were used without further purification.

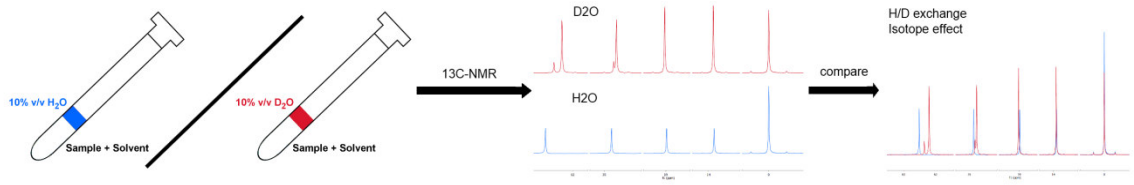

Figure 2-10 Schematic explanation to describe the way from the preparation of the samples to the presented results.

Each sample was measured twice in 500 µl solvent (pyridine, $CDCl_3$ or CD_3OH/CD_3OD), to which either 50 µl H_2O or D_2O were added. When methanol was the solvent of choice, mixtures of CD_3OD and D_2O or CD_3OH and H_2O were used respectively. In each sample 15 mg of a solid or 50 µl of a liquid were dissolved. 10 µl TMS were added to each sample for chemical shift referencing. All NMR spectra were measured on a Bruker AVANCE III 300 MHz spectrometer using a 5 mm TXI probe with z-axis gradients at 300 K. Typically, for proton broadband decoupled ^{13}C-spectra 512 scans with 32 k data points were acquired, using a relaxation delay of 2 seconds. In the case of erythromycin more scans (2048) were recorded. All FIDs were zero-filled to 64k data points after multiplication with an exponential window function using a line-broadening of 1.00 Hz along t_1, prior to Fourier transformation. All processing was done using MestReNova 8.0.0.. A scalar coupling to ^1H was suppressed by applying the “zgpg30” decoupling pulse sequence.

2.3. Summary

To summarize, it was shown that in the three solvents tested all protonated groups could be clearly differentiated from the non-protonated groups and the measurement of the DIS values led to a simpler and faster assignment of the structure. This was especially evident from the results of erythromycin and rutin, where it was shown how well it works even with bigger molecules. Of course, this method cannot be used alone, but also requires other strategies, such as 2D spectra measurements. Nevertheless, it helps to reduce the number of unidentified shifts before moving on to more time-consuming techniques. Additionally you sometimes can already say whether the molecule measured has the right amount of protonated groups or not. To better illustrate the comparison of the different solvents some of the measured chemicals and their results in the different solutions can be found in the appendix. (Figure 6-1) In conclusion, it is increasingly important to have a correct and accurate assignment of the atoms as this can be critical for the interpretation of the data.

3. INLAYS TO IMPROVE THE SIGNAL-TO-NOISE RATIO

3.1. Theoretical

There are many factors in NMR that can improve the signal to noise ratio (SNR). These were physically described very early by Hoult et al..[15] A simple way to improve this ratio is to reduce the sample volume by reducing the diameter of the NMR-tubes.[4,16,17] This can already be realized so far that volumes in the single-digit µl range are achieved as V_{obs}.[17,18] Another possibility is to improve the geometry. It has already been shown that a rectangular shape provides better properties than a round shape.[19,20] In higher salt concentrations of 300 mM NaCl an improvement of factor two of the SNR per volume could be determined.[19] Whereas in 100 mM NaCl a maximum improvement of 15% was theoretically calculated. This improvement comes from the fact, that the RF-power is not homogenous and the edge areas of the circular NMR-tube have the higher power dissipation perpendicular to the B_1 field.[20]

There are already several examples where 3D printed objects were used in a magnetic environment.[18,21–23] A good example from medicine is that an apparatus was printed to fix mice in a MRI measurement to improve the image taken.[21] In NMR, 3D-printing was used to build specific NMR cells to better degas samples directly[22], to improve the NMR sensors and reduce their size[18] or to directly print a NMR-tube plus spinner already filled with the reaction samples inside an inert atmosphere.[23]

Our approach was to combine these two pieces of information to create an inlay to improve the SNR without having to rely on more expensive methods or equipment.

3.1.1. Material

3.1.1.1. Acrylonitrile butadiene styrene (ABS)

ABS is a thermoplastic polymer made out of acrylonitrile and styrene, which were polymerized in the presence of polybutadiene. It is for example used to produce LEGO[24] and a common material in 3D-printing. It was also shown, that ABS can be used in mild solvents such as water, hexane, diethyl ether or ethanol, but not in more aggressive solvents such as acetone, acetonitrile, DMSO or THF.[25] To improve the mechanical properties of ABS it can be considered to print the models in an inert nitrogen environment. This would reduce the oxidation process during the printing, which leads to a degradation of the material.[26] It also shows promising results in NMR experiments, since it only shows weak and narrow signals around 130 and 30 ppm.[27]

3.1.1.2. Photoreactive Resin

The photoreactive resin used by Formlabs© ("standard clear Kunstharz") is a mixture of methacrylic acid esters and photoinitiator. It is commonly used in SLA 3D-printers and produces a better resolution than other available printing methods at Fablab©. "Upon post-cure, tensile strength and stiffness exceeds that of injection-molded or 3D-printed ABS."[28] It was also shown, that it could be used in different solvents such as isopropyl alcohol, butyl acetate, isooctane, water, xylene, bleach (~5%NaOCl) or acetic acid (5%).[28] The only counterproductive thing is that it unfortunately gives a lot of signals in NMR.[29] This fact was later ignored in the decision which material should be used and it was hoped that it would not drastically affect the measurements.

3.1.2. Prototype 1

For the first prototype we thought about using a slice selective pulse sequence to find out in which kind of orientation the inlay has to be put into the NMR-tube. At the same time we also wanted to get more information, which kind of hole geometry would give us the best signal for noise improvement. First of the size of the inlay was decided to be 172 mm long and the main part would have a radius of 2.1 mm to fit inside the NMR-tube. With this size we would have 1 mm for a fixation at the top of the inlay and would reach all the way down to the measurement space inside a 5 mm NMR-tube. The measurement space,

where the main part of the inlay should be located, starts 9 mm over the bottom of a 5mm NMR-tube and has a size of 23 mm. With this information it was then decided to make 11 chambers inside the main part, with a thickness of 1 mm and a barrier in between of 1 mm only connected by a 0.5 mm radius cylindrical hole in the middle.
From bottom to top the chambers were:

- a 2 mm wide rectangular hole aligned to the fixation
- a 2 mm wide rectangular hole turned by 90 degrees with respect to the fixation
- a 2 mm wide rectangular hole turned by 45 degrees with respect to the fixation
- a 2 mm wide rectangular hole turned by -45 degrees with respect to the fixation
- a 1 mm wide rectangular hole aligned to the fixation
- a 1 mm wide rectangular hole turned by 90 degrees with respect to the fixation
- a 3 mm wide rectangular hole aligned to the fixation
- a 3 mm wide rectangular hole turned by 90 degrees with respect to the fixation
- a 1.5 mm radius cylindrical hole
- a 1 mm radius cylindrical hole
- a 0.75 mm radius cylindrical hole.

Figure 3-1 Isometric view of the first prototype. The exact dimensions can be found in the text above and in the appendix. The prototype was designed using Autodesk Inventor Professional 2019. (Figure 6-2 and Figure 6-3)

3.1.3. Prototype 2

After the first prototype had been tested, it was decided to produce a second prototype. For this second prototype it was chosen to use the same dimensions as for the first prototype for everything, except the chambers. The single chamber was selected to be a 2 mm wide rectangular hole with a height of 21 mm. This was thought to improve the shimming of the NMR before starting an experiment, which seemed to be the main problem of the first prototype.

Figure 3-2 Isometric view of the second prototype. The dimensions are identical to the first prototype except for the inner chamber. The chamber is a 2 mm wide and 21 mm high rectangular hole. The exact dimensions can be found in the appendix. The prototype was designed using Autodesk Inventor Professional 2019. (Figure 6-2 and Figure 6-3)

3.2. Experimental

The NMR spectra were either measured on a Bruker AVANCE III 300 MHz spectrometer using a 5 mm TXI probe with z-axis gradients at 300 K or on a 3-canal Bruker Avance III 500 MHz using a 5 mm HX or a 5 mm triple resonance probe with z-axis gradients at 300 K. Typically, for proton broadband decoupled ^{13}C-spectra 512 scans with 16k data points and a spectral size of 64k were acquired, using a relaxation delay of 2 seconds. For ^{1}H-spectra 16 scans were taken with 16k data points, a spectral size of 32k and using a relaxation delay of 2 seconds. The slice selective measurements were taken using the zgslice.zk sequence. 128 scans were taken for 16k data points, a spectral size of 32k and using a relaxation delay of 1 second. All processing was done using MestReNova 8.0.0..

3.2.1. Material test

To test out in which simple solvent the inlays could be tested a sample print from Formlabs© was ordered. After receiving the clear rook (chess piece) the battlements were cut off with a knife to approximately same seized pieces. These pieces were then weighed and put in different solvents. After 23 h the samples were simply dried with tissue, weighed (1. control) and put back into their solvents. This time they were put into an ultrasonic bath for 15 min before letting them rest in the solvent for 92 h. The samples were then dried again with tissues and put into new clean vials, which were left open and standing in the laboratory hood. 5.5 h later they were put into a drying cabinet at 60°C for 19 h before weighing them (2. control). Before undergoing the last control (3. control) the samples were again put into their corresponding solvent for 142 h, dried in the hood for 3.5 h and dried in the drying cabinet at 60°C for 20 h. For the last control the stability of the sample was also tested by applying a bit of pressure with pincers. The results of the controls and which solvents were tested can be found in Table 4.

Table 4 The weights of the samples after each control and their corresponding solvents. All numbers are given in[mg].

solvents	start	1. control	2. control	3. control	pressure
D_2O	22.26	22.49	21.82	21.77	hard, solid
EtOH	27.23	30.21	25.32	24.83	hard, solid
THF	30.62	29.12	22.66	25.15	brittle, breaks
Pyridin	25.69	27.10	22.38	16.05	brittle, breaks
$CDCl_3$	19.14	31.44	21.51	21.66	brittle, breaks
DMF	25.86	31.75	25.62	25.12	hard, solid
Aceton	24.46	26.54	22.80	21.70	hard, solid
Acetonitril	28.30	31.69	27.96	27.81	hard, solid
DMSO	26.40	28.71	26.32	28.74	brittle, breaks

With these results it was decided to use ethanol dissolved in D_2O to test the efficiency of the inlays in an NMR experiment.

3.2.2. Workup

For the printing the prototypes designed in Autodesk Inventor Professional 2019, were sent to the workers at Fablab©. After discussing with the experienced workers from there, which material would give the best result it was concluded, that "standard clear Kunstharz" (Photoreactive Resin) would be used instead of ABS. This decision was made, because

ABS would be too flexible and the printing method would not be as detailed as we would need it. The machine used was a Form 2 SLA 3D-printer from Formlabs©.

After receiving the prototype from Fablab© it first had to be separated from the stability cage, which was needed to print such a fragile form. This was done using a stanley knife and a nipper. Afterwards the outside of the prototype was polished to better fit inside the NMR-tube and the main hole connecting all the chambers was drilled after to ensure that all chambers can be filled from the top. Next the prototype was cleaned with pressured air, an ultrasonic bath, distilled water and ethanol to make sure that no particles remain inside. After finishing all the steps the inlays were ready for the measurements.

3.2.3. Measurements

For the first measurements it was decided to use a solution of ~0.3 ml (a drop) ethanol added to 2.5 ml D_2O. 250 µl of this mixture was taken to fill up the chambers of the first prototype inside the NMR-tube. At first it was not possible to acquire a resolved spectrum, because the automatic shimming failed. After testing around and shimming it manually it was at least possible to get a spectrum with three signals (two signals corresponding to ethanol and one signal for the solvent) and a big drift beneath it. (Figure 3-3a)

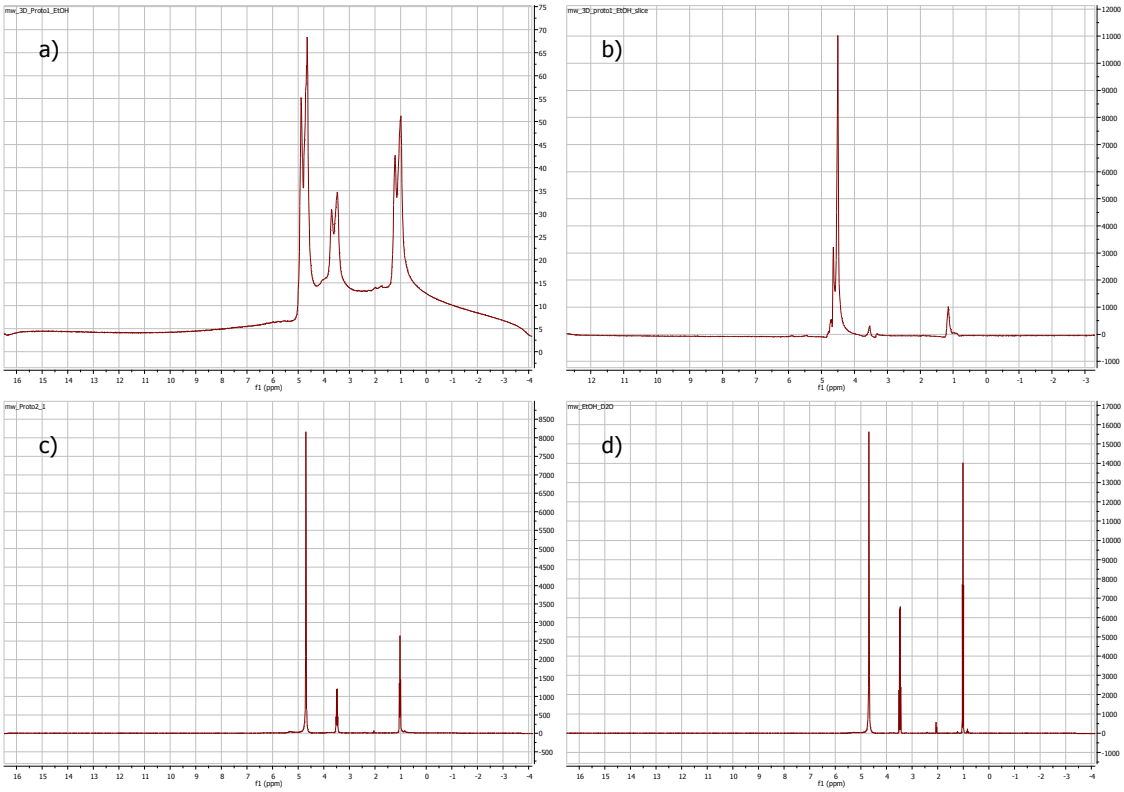

Figure 3-3 Spectra of ethanol in D_2O. a) ^1H spectrum manually shimmed with Prototype 1. b) Slice selective spectrum manually shimmed with Prototype 1. c) ^1H spectrum automatically shimmed with Prototype 2. d) ^1H spectrum without the addition of an inlay.

The slice selective spectrum, which can be seen in Figure 3-3b shows a much more promising result but is still heavily affected by the inhomogeneity, resulting from the geometry of the prototype. To overcome this problem prototype 2 was measured in the same environment. As can be seen by comparing Figure 3-3b and c this improves the resolution of the spectrum by a lot. But it is still not as good as a measurement of just the sample without the addition of an inlay would be. (Figure 3-3d) The same result was found for the comparison of the ^{13}C-spectra. Interestingly, the slice selective spectra were nearly the same with or without the use of Prototype 2, but they were still less sensitive than a normal ^{1}H-spectra.

Finally it was tried to measure and compare a glucose solution. However the results were no better than for ethanol, so this project was temporarily closed at this point.

3.3. Summary

The results have concluded that it would be possible to use inlays in NMR-tubes in certain solvents. The next approach would be to improve the geometry of the inlay and to better lock it in place inside the NMR-tubes. In addition, it might be a good idea to have the entire NMR-tube and spinner printed in a 3D printer to see whether this would help with homogeneity. This could also be done with ABS, which seems to show better NMR compatibility.[18,21] Another approach would be to run the sample measurements in the presence of higher salt concentrations, as it better shows the improvement in SNR.[19,20] Furthermore, it would be good to get an apparatus that ensures that the NMR-tube reaches the magnetic field in a certain orientation.

4. USE OF CYCLODEXTRIN-DERIVATES AS CHIRAL SOLVATING AGENTS

4.1. Theoretical

The first record of cyclodextrin (CD) dates back to 1891.[30] Since that time, there has been a lot of new insight into the synthesis and complex binding properties of this molecule. CDs are cyclic oligosaccharides composed of six (α), seven (β) or eight (γ) α-1,4-glucosidically linked glucose molecules. Particularly striking is the frustoconical structure of CD (Figure 4-1) and that the interior is hydrophobic, while the outside is hydrophilic. This property allows the uptake of hydrophobic molecules to form a complex and to solubilize them in a hydrophilic solvent. That makes it one of the main reasons why CD became interesting for almost every chemical direction.[31,32]

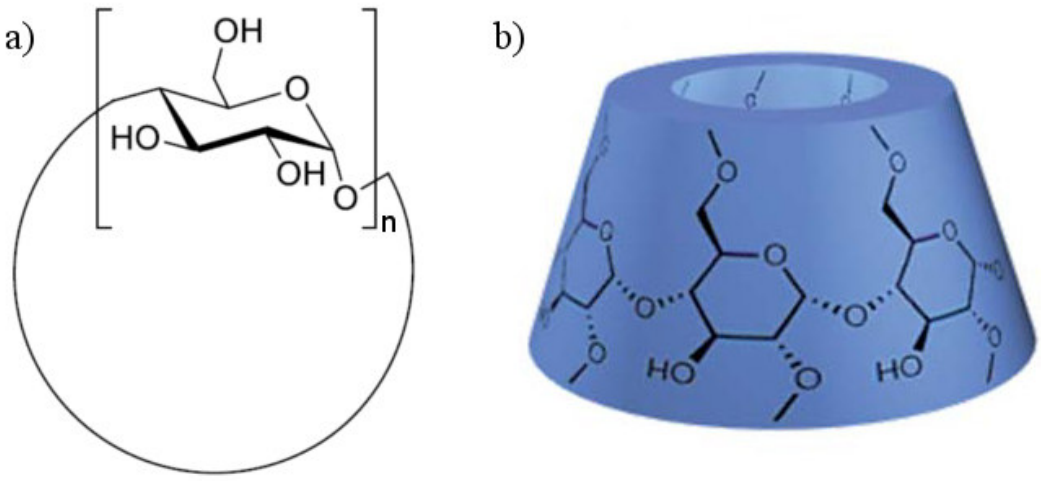

Figure 4-1 a) CD from α-1,4-glucosidically linked glucose units (n=6(α),7(β),8(γ)) b) the resulting frustoconical structure (the picture comes from the Ritter group[32])

Since CD is a chiral molecule, the incorporation of chiral molecules also forms a diastereomeric inclusion complex, which may have different physical properties. These can be, for example, used in RAMAN scatter experiments[33], in neurochemistry to improve microdialysis[34], in a voltammetric method to selectively detect uric acid[35], in crystallography to determine the absolute configuration of guest molecules[36], in high pressure liquid chromatography as an additive to the mobile phase for a faster enantiomeric separation[37] or in different NMR experiments.[5,6,38–42]

4.1.1. CDs in NMR

Of particular interest to us is the previous use in NMR. It has been shown that CDs can be used as chiral solvating agents to establish enantiomeric purity.[38] Complex formation with the guest molecules also leads to a change in the ^{1}H spectrum, which can confirm this reaction.[40,41] With the help of ROESY experiments it was also possible to show which part of the guest molecule binds to the CD.[39,42] This was further used to show that molecules with different chirality can sometimes even have a different orientation in the complex[5] and to determine the optical purity of synthesized molecules, for example, (S)-mandelonitrile.[6]

4.2. Experimental

The chemicals were purchased from Sigma-Aldrich (St. Louis, MO, USA) at >98% purity and were used without further purification or borrowed from the working group of Prof. Kroutil.

The NMR spectra were either measured on a Bruker AVANCE III 300 MHz spectrometer using a 5 mm TXI probe with z-axis gradients at 300 K or on a 3-channel Bruker Avance III 500 MHz using a 5 mm HX or a 5 mm triple resonance probe with z-axis gradients at 300 K. ~30 µl TMS were added to each sample for chemical shift referencing. Typically, for proton broadband decoupled ^{13}C-spectra 1024 scans with 32 k data points were acquired with a spectral size of 64k and using a relaxation delay of 2 seconds. For ^{1}H-spectra 16 scans were taken with 32k data points, a spectral size of 64k and using a relaxation delay of 1 seconds. All processing was done using MestReNova 8.0.0.. A scalar coupling to ^{1}H was suppressed by applying the “zgpg30” decoupling pulse sequence.

The IR-measurements were taken utilizing a Bruker Alpha IR spectrometer equipped with an ATR unit.

The "inert" argon atmosphere was rather complicated, because no argon line was available inside the laboratory. This kind of atmosphere was simulated by filling a balloon with argon and connecting it with a short pipe to the apparatus. To improve this kind of trick the connection was also sealed with a thick layer of parafilm.

4.2.1. Synthesis of 1-[(4-Methylphenyl)sulfonyl]-1*H*-imidazol **(a)**

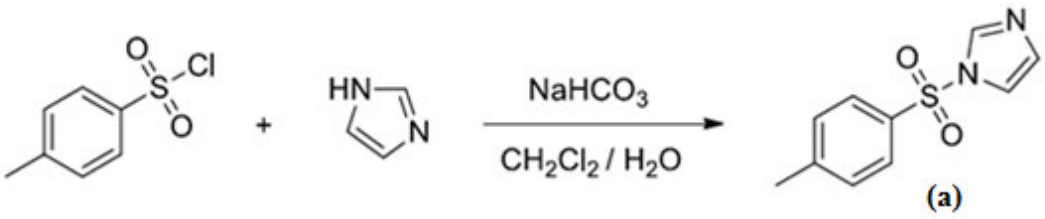

The compound was synthesized analogously to Tan et al.[43]

In a 250 ml Erlenmeyer flask with magnetic stirrer 3.30 g (48.5 mmol, 1 equiv.) imidazol and 9.90 g (51.9 mmol, 1.07 equiv.) p-toluenesulfonyl chloride were dissolved in 39 ml CH_2Cl_2. Subsequently, a solution of 5.02 g (59.8 mmol, 1.23 equiv.) $NaHCO_3$ in 64 ml H_2O and 0.71 ml (5.1 mmol, 0.11 equiv.) Triethylamine were added and the resulting two-phase system was stirred vigorously at room temperature. After 4 h (reaction control of the organic-phase by ^{1}H-NMR spectroskopy in $CDCl_3$) the organic-phase was separated, dried over $MgSO_4$, filtered and evaporated to a volume of ~15 ml. The concentrated solution was layered with approximately 5 ml n-hexane and placed in the refrigerator overnight for crystallization. The crystallized product was filtered by suction with a glass frit and washed two times with n-hexane before drying it under vacuum inside a desiccator.

Yield: 6.20 g (27.9 mmol, 58 %), white/colorless needlelike crystals

^{1}H-NMR (500.13 MHz, $CDCl_3$): δ = 8.00 (t, 1H), 7.82 (d, ^3J = 8.4 Hz, 2H), 7.35 (d, ^3J = 8.1 Hz, 2H), 7.28 (t, ^3J = 1.4 Hz, 1H), 7.07 (dd, 1H), 2.43 (s, 3H).

^{13}C-NMR (125.77 MHz, $CDCl_3$): δ = 146.3, 136.7, 135.1, 131.4, 130.4, 127.4, 117.4, 21.7.

4.2.2. Synthesis of 6-*O*-*p*-toluenesulfonyl-6-desoxy-β-cyclodextrin **(2)**

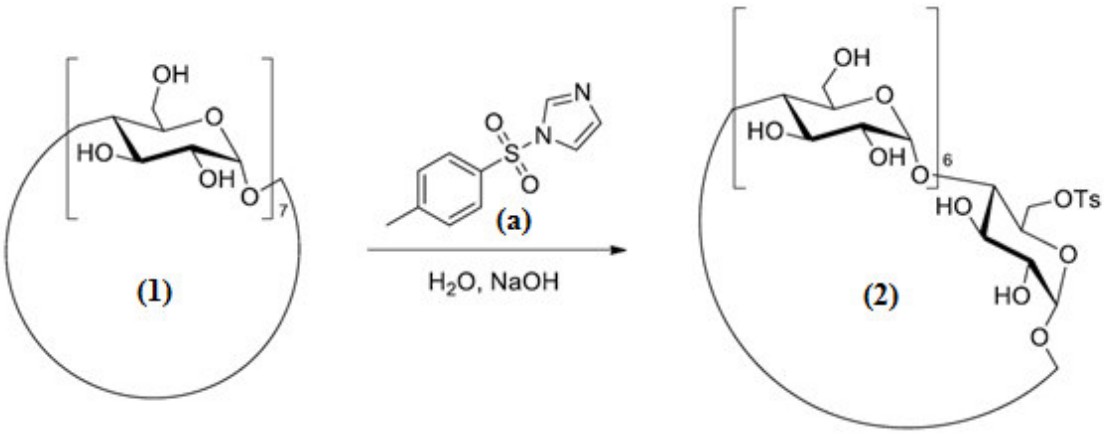

The compound was synthesized analogously to Byun et al.[44]

In a 250 ml round-bottomed flask with magnetic stirrer, 7.72 g (6.8 mmol, 1 equiv.) **(1)** were dissolved in 175 ml dist. H_2O under stirring and heating to 60°C. After letting it cool down to room temperature (still stirring), 6.20 g (27.9 mmol, 4.1 equiv.) **(a)** were added to the milky solution. The solution was then stirred for 2 h before a solution of 3.45 g NaOH in 10 ml H_2O were added over 20 min. 10 min after the addition is completed unreacted **(a)** was separated by filtering with a glass frit. 9.27 g NH_4Cl were added to the remaining solution under swirling to quench the reaction. The volume was then reduced by rotating it at 70-80°C under vacuum until **(2)** starts to precipitate. The solution was then filtrated through a sintered glass funnel without adding vacuum. After washing the collected solid two times with 20 ml ice water and one time with 40 ml acetone it was dried to constant weight over $CaCl_2$ inside a vacuum desiccator.

Yield: 1.50 g (1.2 mmol, 18 %), white powder

^{1}H-NMR (300.13 MHz, DMSO): δ = 7.76 (d, 2H), 7.44 (d, 2H), 5.73 (m, ~14H), 4.84 (m, 5H), 4.77 (m, 2H), 4.52 (m, 5H), 4.35 (dd, 2H), 4.19 (dd, 1H), 3.58 (m, +H_2O), 2.43 (s, 3H)

^{13}C NMR (75.48 MHz, DMSO): δ = 144.66, 132.50, 129.78, 127.43, 101.87, 81.48, 72.89, 72.31, 71.89, 59.77, 40.18, 39.90, 39.62, 39.34, 39.06, 38.79, 38.51, 21.06.

IR [cm^{-1}]: 3288.64 (OH-), 2923.69 (CH-), 1648.86/1597.90 (C=N-), 1022.71 (OH-)

4.2.3. Synthesis of mono-6-deoxy-6-azido-β-cyclodextrin **(3)**

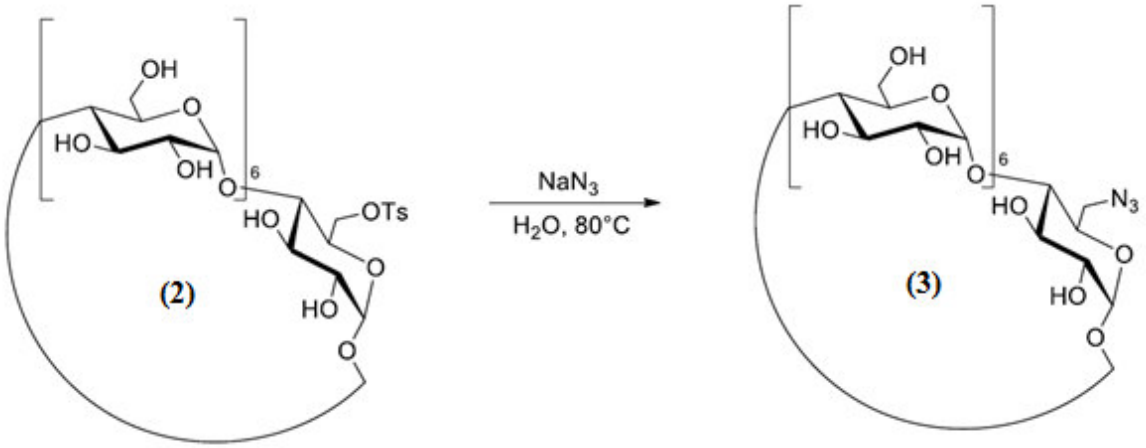

Procedure A.

The compound was synthesized similarly to Ondrusek et al.[45]

In a 100 ml round-bottomed flask with magnetic stirrer, 1.00 g (0.78 mmol, 1 equiv.) **(2)** and 0.26 g (3.97 mmol, 5.1 equiv.) NaN_3 were added into 20 ml dist. H_2O. This solution was stirred and heated to 80°C for 14 hours. While still hot the reaction mixture was filtered through a sintered glass funnel to remove hydrolyzed material, which are insoluble in water. The filtrate was then added to 50 ml acetone, causing a white solid to crash out of solution. The solid was then collected by vacuum filtration and washed with a bit of acetone. This procedure was done again two days later to get a higher yield.

Yield: 0.73 g (0.63 mmol, 81 %), white powder

Procedure B.

The compound was synthesized similarly to Petter et al.[46]

In a 100 ml round-bottomed flask with magnetic stirrer, 0.50 g (0.39 mmol, 1 equiv.) **(2)** were suspended in 2 ml dry DMF after warming to 65°C. 0.03 g (0.18 mmol, 0.46 equiv.) KI and 0.26 g (3.97 mmol, 10.2 equiv.) NaN_3 were added to the now homogenous solution. The reaction mixture was then stirred at 65°C for 20 hours. Afterwards it was cooled to room temperature and the salt was removed with an ion exchanging resin. After adding 70 ml acetone a white precipitate was produced. The solid was then collected by vacuum filtration and dried over night inside a vacuum desiccator.

Yield: 0.28 g (0.24 mmol, 62 %), white powder

^{1}H-NMR (500.13 MHz, DMSO): δ = 5.71 (dd, 14H), 5.62 (s, 1H), 4.87 (d, 1H)), 4.82 (d, 6H), 4.53 (m, 2H), 4.46 (d, 5H), 3.75 (d, 1H), 3.63 (m, $+H_2O$), 3.56 (d, 8H), 3.38 (m, $+H_2O$) 2.08 (s, 6H)

^{13}C-NMR (125.77 MHz, DMSO): δ = 101.75, 81.37, 81.22, 72.84, 72.21, 72.01, 71.83, 59.72, 30.50

IR [cm^{-1}]: 3338.67 (OH-), 2924.08 (CH-), 2103.49 (N_3-), 1025.86 (OH-)

4.2.4. Synthesis of mono-6-(N,N,N-trimethylammonio)-6-deoxy-β-cyclodextrin **(4)**

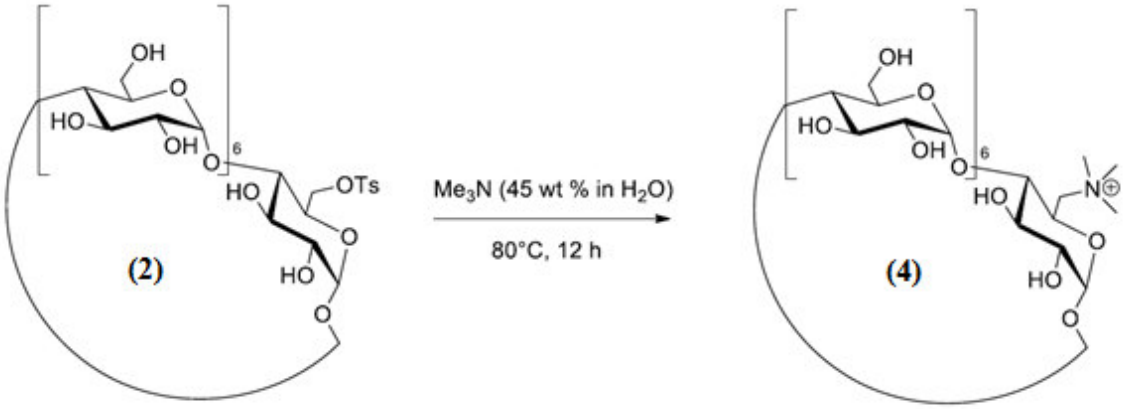

The compound was synthesized similarly to Popr et al.[47]

In a 100 ml round-bottomed flask with magnetic stirrer, 0.50 g (0.39 mmol, 1 equiv.) **(2)** were added to an aqueous solution of 3.80 ml (0.04 mmol, 0.10 equiv.) trimethylamine (45 wt %). This reaction mixture was stirred at 80°C for 12 hours. The mixture was then separated on a column of strong cation exchange resin in hydrogen form (Dowex 50). The column was washed at first with 100 ml H_2O to remove possible byproducts and then with aqueous NH_4HCO_3 3 wt % (100 mL) to get the product. The salts were removed by repeated vacuum evaporation (thermal decomposition of the salts) with H_2O (2 x 30 ml). An attempt at collecting the product, by adding 60 ml acetone, to produce a white precipitate, and purifying the solid by vacuum filtration and drying it over night inside a vacuum desiccator, was made.

Yield: 0%

Due to unknown problems in the purification no product could be isolated.

4.2.5. Synthesis of mono-6-((2-(Dimethylamino)-1-(methyl)ethyl)amino)-6-deoxy-β-cyclodextrin **(5)**

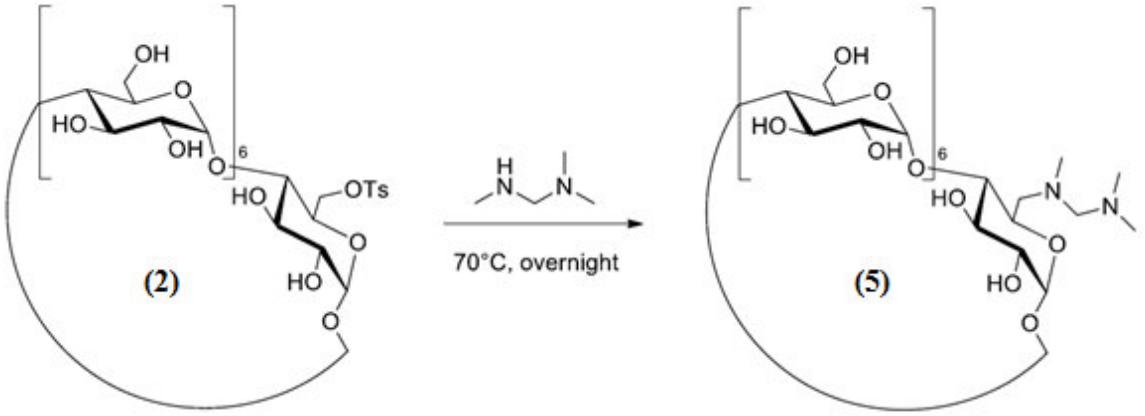

The compound was synthesized similarly to Popr et al.[47]

In a 50 ml round-bottomed flask with magnetic stirrer, 0.50 g (0.39 mmol, 1 equiv.) **(2)** were dissolved with stirring in 3 ml (2.38 g, 23.3 mmol, 59.7 equiv.) N,N,N'-trimethylethane-1,2-diamine, under "inert" atmosphere of argon. Once **(2)** is completely dissolved the solution is heated to 70°C and stirred overnight. The reaction mixture changed to a dark brown colour and was vacuum distilled at room temperature to recover unreacted N,N,N'-trimethylethane-1,2-diamine. The brown residue was dissolved in minimum amount of water (~1 ml) and precipitated by adding it dropwise to 60 ml n-propanol. The solid was then collected by filtration through a sintered glass funnel under vacuum and drying it over night inside a vacuum desiccator at room temperature.

Yield: 0.30 g (0.25 mmol, 63 %), white powder

^{1}H-NMR (500.13 MHz, DMSO): δ = 5.94 (d, 1H), 5.71 (m, 14H), 4.83 (dt, 8H), 4.53 (s, 1H), 4.45 (s, 4H), 3.62 (m, 29H), 3.36 (m, +H_2O), 2.37 (dt, 1H), 2.26 (dq, 3H), 2.17 (s, 3H), 2.08 (s, 3H), 2.07 (s, 6H)

^{13}C-NMR (125.77 MHz, DMSO): δ = 102.00, 101.83, 101.40, 83.99, 81.33, 81.05, 73.17, 72.84, 72.63, 72.30, 72.24, 72.07, 71.83, 71.73, 70.12, 62.29, 59.67, 56.79, 55.72, 45.21, 43.06, 25.45, 10.26

4.2.6. Synthesis of mono-6-amino-6-deoxy-β-cyclodextrin **(6)**

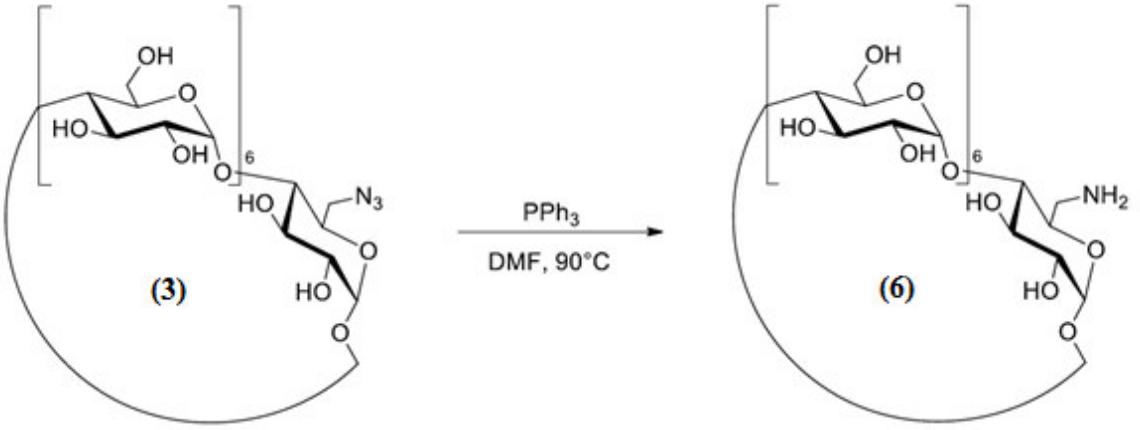

The compound was synthesized similarly to Tang et al.[48]

In a 50 ml Erlenmeyer flask with magnetic stirrer 0.2 g (0.17 mmol, 1 equiv.) **(3)** and 0.1 g (0.38 mmol, 2.2 equiv.) triphenylphosphine were stirred in 10 ml DMF at room temperature for 2h. Afterwards 1 ml of H_2O was added to the reaction mixture and refluxed at 90°C for 3h. To collect the white solid acetone was added dropwise to cause precipitation. The solution was then filtered through a glass frit and the solid was washed with acetone. To dry the product it was placed inside a vacuum desiccator at room temperature overnight.

Yield: 0.17 g (0.15 mmol, 88 %), white powder

^{1}H-NMR (500.13 MHz, DMSO): δ = 5.69 (m, 27H), 4.84 (m, 14H), 4.46 (s, 9H), 3.85 (t, 2H), 3.62 (m, +HDO), 3.37 (m, +H_2O), 2.82 (dd, 2H), 2.08 (s, 3H), 1.91 (s, 1H), 1.77 (s, 1H)

^{13}C-NMR (125.77 MHz, DMSO): δ = 101.82, 81.45, 72.87, 72.28, 71.87, 59.76, 30.53

4.3. Combination with target guest molecules

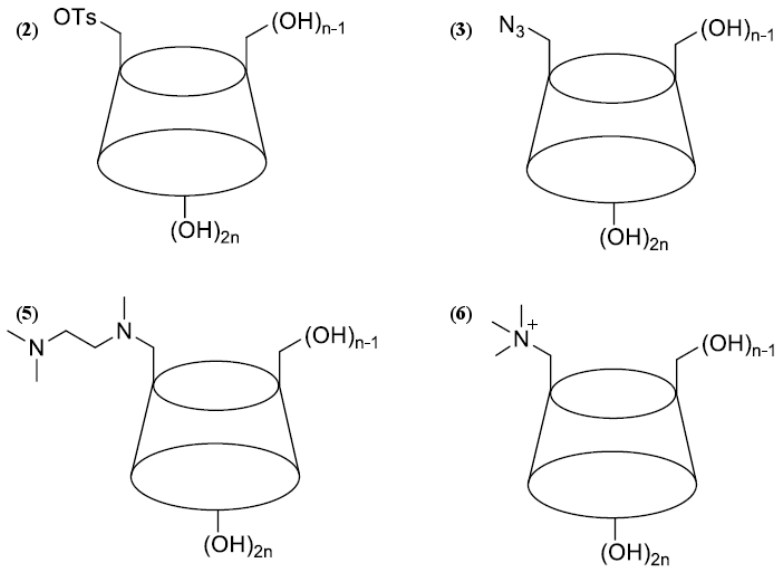

Figure 4-2 Target host molecules, which were synthesized in chapter 4.2.

The solutions of the β-cyclodextrin derivates were prepared by first weighing them and then dissolving them with 3 ml d6-DMSO.

Table 5 Weighing of the β-cyclodextrin derivates in [mg], in 3 ml d6-DMSO.

(2)	(3)	(5)	(6)
251.5	173.6	204.8	100.5

Afterwards ~20 mg of the guest molecules, mandelic acid (MDA), 2-pantolactone (PL), 1-phenyl-1,2-ethanediol (PED) and mandelonitrile (MON), were put into a sampling vial.

Table 6 Weighing of the guest molecules in [g] for the four tested β-cyclodextrin derivates.

	MDA	PL	PED	MON
(2)	0.019	0.022	0.032	0.025
(3)	0.026	0.029	0.023	0.025
(5)	0.022	0.019	0.020	0.027
(6)	0.026	0.023	0.020	0.024

600 µl of the appropriate solution were added to the prepared samples of the guest molecules before measuring it with the NMR. These spectra were then compared with previously collected spectra, which were measured without the addition of a β-cyclodextrin derivate.

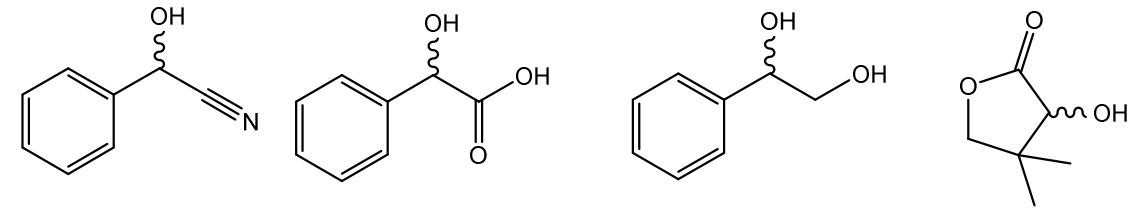

Mandelonitrile (MON) Mandelic acid (MDA) 1-phenylethane-1,2-diol (PED) Pantolacton (PL)

Figure 4-3 Target guest molecules, which were tried to be combined with the host molecules.

Unfortunately, no complex formation was found in the combinations of host and guest molecules. This finding was justified by the fact that no change in the ^{1}H spectrum could be observed, which should occur in a complex formation.[40] Furthermore, no splitting of a signal was observed, which would have signaled the enantiomeric separation of the guest molecules.

Table 7 Detailed ^{1}H-NMR results of pure PL and its combination with the CD-derivatives.

PL	0.91	1.08	3.93	4.08	5.93
	s 3H	s 3H	s 2H	d (3.6 Hz) 1H	d (4.6 Hz) 1H
(2)	0.90	1.08	3.93	4.09	5.97
	s 3H	s 3H	s 2H	d (3.6 Hz) 1H	d (5.2 Hz) 1H
(3)	0.90	1.07	3.92	4.08	5.94
	s 3H	s 3H	s 2H	s 1H	s 1H
(5)	0.90	1.07	3.92	4.07	5.94
	s 3H	s 3H	s 2H	s 1H	s 1H
(6)	0.90	1.07	3.92	4.08	5.95
	s 3H	s 3H	s 2H	s 1H	s 1H

The exact results of the combination of PL with the host molecules are given in Table 7. In addition, Figure 4-4 shows that the signals of PED in all combinations with CD-derivatives are almost identical to the pure spectrum of PED. The signal around 4.8 ppm can be ignored as it is very likely to be the signal of HDO.

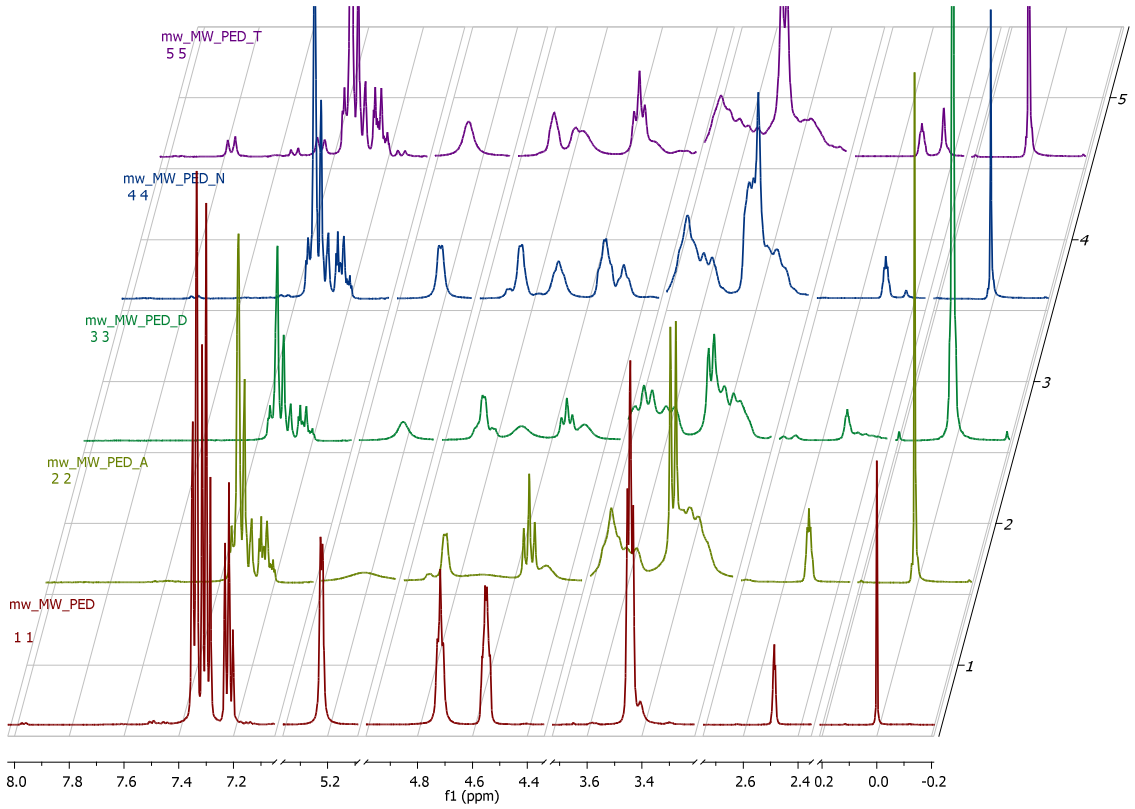

Figure 4-4 Stacked spectra of pure PED [red] and it's combinations with (2) [violet], (3) [blue], (5) [green] and (6) [yellow]. The spectra show that they are almost identical with respect to PED. The signal at 0 ppm comes from TMS and the signal around 4.8 ppm should be the HDO peak from D_2O.

4.4. Summary

From these results one can conclude that it is highly improbable for an universal CD-derivative that can be used as an addition to any chiral molecule to determine its purity to exist. Nevertheless, it is of course possible to find such a solution for a defined problem, but it probably needs a very good understanding of the matter as well as a bit of luck. Moreover, it would be advisable for further experiments in this direction to put a stronger emphasis on the syntheses in order to obtain products with a higher purity. Lastly, purifying the guest molecules before combining them with the host molecules is highly recommended.

5. LITERATURE

(1) Dorn, H. C. *Analytical Chemistry* **1984**, *56*, 747A-758A.
(2) Albert, K. *Journal of Chromatography A* **1995**, *703*, 123–147.
(3) Pfeffer, P. E.; Valentine, K. M.; Parrish, F. W. *Journal of the American Chemical Society* **1979**, *101*, 1265–1274.
(4) Voehler, M. W.; Collier, G.; Young, J. K.; Stone, M. P.; Germann, M. W. *Journal of Magnetic Resonance* **2006**, *183*, 102–109.
(5) Negi, S.; Terai, K.; Kano, K.; Nakamura, K. *J. Chem. Research* **1998**, *(S)*, 750–751.
(6) Hickel, A.; Gradnig, G.; Schall, M.; Zangger, K.; Griengl, H. *Spectrochimica Acta Part A: Molecular and Biomolecular Spectroscopy* **1997**, *53*, 451–455.
(7) Batiz-Hernandez, H.; Bernheim, R. A. *Progress in Nuclear Magnetic Resonance Spectroscopy* **1967**, *3*, 63–85.
(8) Altman, L. J.; Laungani, P.; Gunnarsson, G.; Wennerstrom, H.; Forsen, S. *Journal of the American Chemical Society* **1978**, *100*, 8264–8266.
(9) Kenneth Ladner, H.; Led, J. J.; Grant, D. M. *Journal of Magnetic Resonance (1969)* **1975**, *20*, 530–534.
(10) Feeney, J.; Partington, P.; Roberts, G. C. . *Journal of Magnetic Resonance (1969)* **1974**, *13*, 268–274.
(11) Pfeffer, P. E.; Parrish, F. W.; Unruh, J. *Carbonhydrate Research* **1980**, *84*, 13–23.
(12) Zheglova, D. K.; Genov, D. G.; Bolvig, S.; Hansen, P. E. *Acta chemica scandinavia* **1997**, No. 51, 1016–1023.
(13) Newmark, R. A.; Hill, J. R. *Organic Magnetic Resonance* **1980**, *13*, 40–44.
(14) Capon, B.; Rycroft, D. S.; Watson, T. W.; Zucco, C. *Journal of the American Chemical Society* **1981**, *103*, 1761–1765.
(15) Hoult, D. .; Richards, R. . *Journal of Magnetic Resonance (1969)* **1976**, *24*, 71–85.
(16) Robosky, L. C.; Reily, M. D.; Avizonis, D. *Analytical and Bioanalytical Chemistry* **2007**, *387*, 529–532.
(17) Schlotterbeck, G.; Ross, A.; Hochstrasser, R.; Senn, H.; Kühn, T.; Marek, D.; Schett, O. *Analytical Chemistry* **2002**, *74*, 4464–4471.
(18) Saggiomo, V.; Velders, A. H. *Advanced Science* **2015**, *2*, 1500125.
(19) Takeda, M.; Hallenga, K.; Shigezane, M.; Waelchli, M.; Löhr, F.; Markley, J. L.; Kainosho, M. *Journal of Magnetic Resonance* **2011**, *209*, 167–173.
(20) de Swiet, T. M. *Journal of Magnetic Resonance* **2005**, *174*, 331–334.
(21) Herrmann, K.-H.; Gärtner, C.; Güllmar, D.; Krämer, M.; Reichenbach, J. R. *Medical Engineering & Physics* **2014**, *36*, 1373–1380.
(22) Causier, A.; Carret, G.; Boutin, C.; Berthelot, T.; Berthault, P. *Lab on a Chip* **2015**, *15*, 2049–2054.
(23) Lederle, F.; Meyer, F.; Kaldun, C.; Namyslo, J. C.; Hübner, E. G. *New Journal of Chemistry* **2017**, *41*, 1925–1932.
(24) May, P. July 31, 2017.
(25) Gordeev, E. G.; Degtyareva, E. S.; Ananikov, V. P. *Russian Chemical Bulletin* **2016**, *65*, 1637–1643.
(26) Lederle, F.; Meyer, F.; Brunotte, G.-P.; Kaldun, C.; Hübner, E. G. *Progress in Additive Manufacturing* **2016**, *1*, 3–7.
(27) Lederle, F.; Kaldun, C.; Namyslo, J. C.; Hübner, E. G. *Helvetica Chimica Acta* **2016**, *99*, 255–266.
(28) Formlabs© *FLGPCL03 material properties - standard resins: Photopolymer Resin for Form 2 and Form1+ 3D Printers* **2016**

(29) Elomaa, L.; Teixeira, S.; Hakala, R.; Korhonen, H.; Grijpma, D. W.; Seppälä, J. V. *Acta Biomaterialia* **2011**, *7*, 3850–3856.
(30) Villiers, A. *Compt. Rend. Acad. Sci* **1891**, *112*, 536–538.
(31) Szejtli, J. *Chemical Reviews* **1998**, *98*, 1743–1754.
(32) Zhou, J.; Ritter, H. *Polymer Chemistry* **2010**, *1*, 1552.
(33) Xie, Y.; Wang, X.; Han, X.; Xue, X.; Ji, W.; Qi, Z.; Liu, J.; Zhao, B.; Ozaki, Y. *The Analyst* **2010**, *135*, 1389.
(34) Khramov, A. N.; Stenken, J. A. *The Analyst* **1999**, *124*, 1027–1033.
(35) Wang, Z.; Wang, Y.; Luo, G. *The Analyst* **2002**, *127*, 1353–1358.
(36) Elasaad, K.; Alkhatib, R.; Hennebelle, T.; Norberg, B.; Wouters, J. *Crystals* **2012**, *2*, 1441–1454.
(37) Ma, S.; Shen, S.; Haddad, N.; Tang, W.; Wang, J.; Lee, H.; Yee, N.; Senanayake, C.; Grinberg, N. *Journal of Chromatography A* **2009**, *1216*, 1232–1240.
(38) Uccello-Barretta, G.; Balzano, F.; Pertici, F.; Jicsinszky, L.; Sicoli, G.; Schurig, V. *European Journal of Organic Chemistry* **2008**, *2008*, 1855–1863.
(39) Ali, S. M.; Upadhyay, S. K. *Journal of Inclusion Phenomena and Macrocyclic Chemistry* **2008**, *62*, 161–165.
(40) Casy, A. F.; Mercer, A. D. *Magnetic Resonance in Chemistry* **1988**, *26*, 765–774.
(41) Marangoci, N.; Mares, M.; Silion, M.; Fifere, A.; Varganici, C.; Nicolescu, A.; Deleanu, C.; Coroaba, A.; Pinteala, M.; Simionescu, B. C. *Results in Pharma Sciences* **2011**, *1*, 27–37.
(42) Schneider, H.-J.; Hacket, F.; Rüdiger, V.; Ikeda, H. *Chemical Reviews* **1998**, *98*, 1755–1786.
(43) Tan, T.; Tan, T.; Ng, S.; Wang, Y.; Xiao, Y. *Protocol Exchange* **2011**.
(44) Byun, H.-S.; Zhong, N.; Bittman, R. *Organic Syntheses* **2000**, *77*, 225.
(45) Ondrusek, B. A.; Chung, H. *ACS Omega* **2017**, *2*, 3951–3957.
(46) Petter, R. C.; Salek, J. S.; Sikorski, C. T.; Kumaravel, G.; Lin, F. T. *Journal of the American Chemical Society* **1990**, *112*, 3860–3868.
(47) Popr, M.; Hybelbauerová, S.; Jindřich, J. *Beilstein Journal of Organic Chemistry* **2014**, *10*, 1390–1396.
(48) Tang, W.; Muderawan, I. W.; Ong, T.-T.; Ng, S.-C. *Tetrahedron: Asymmetry* **2007**, *18*, 1548–1553.

6. APPENDIX

DIS	Lösungsmittel	C-1	C-2	C-3	C-4	C-5	C-6	C-7	C-8	C-9	C-10	C-11	C-12
Butan-2,3-diol	MeOD	0,05	0,09										
	CDCl3	0,06	0,12										
	Pyridin	0,06	0,11										
Butan-1-ol	MeOD	0,10	0,02	-0,01	0,00								
	CDCl3	0,16	0,05	-0,03	-0,01								
	Pyridin	0,12	-0,02	-0,03	-0,01								
iso-Butanol	MeOD	0,13	0,05	0,00									
	CDCl3	0,15	0,04	-0,01									
	Pyridin	0,13	0,05	0,01									
2-(2-Ethoxyethoxy)ethanol	MeOD	0,12	0,03	0,00	0,00	0,00	0,01						
	CDCl3	0,12	0,01	0,00	0,00	0,00	0,00						
	Pyridin	0,12	0,04	0,01	0,01	0,00	0,01						
2-Phenoxyethanol	MeOD	0,06	-0,01	-0,05	-0,03	-0,02	-0,02						
	CDCl3	0,14	0,02	0,01	0,00	0,00	0,00						
	Pyridin	0,11	0,04	0,00	0,00	0,00	0,00						
1,2;5,6-Di-O-isopropylglucofuranose	MeOD	-0,02	0,00	0,06	0,01	-0,02	-0,01	-0,01	0,00	0,00	0,00	-0,01	-0,01
	CDCl3	-0,01	0,03	0,10	0,01	-0,04	-0,01	0,01	-0,01	0,00	0,00	0,00	-0,10
	Pyridin	-0,01	0,01	0,09	0,02	-0,01	-0,02	0,01	0,00	-0,01	0,00	0,00	-0,01
Ethylen glycol dimethylether	MeOD	0,00	0,00										
	CDCl3	0,00	0,00										
	Pyridin	0,00	0,00										
1,4-Benzodioxan-6-amine	MeOD	-0,01	0,00	-0,01	0,00	0,09	0,01	-0,01	-0,04				
	CDCl3	-0,01	0,00	0,00	0,00	0,11	0,02	0,00	-0,02				
	Pyridin	0,01	0,01	0,01	0,00	0,13	0,02	0,01	-0,03				
1-Adamantylamine	MeOD	0,13	0,09	-0,01	0,02								
	CDCl3	0,22	0,06	-0,01	0,01								
	Pyridin	0,21	0,08	-0,01	0,01								
Benzylamine	MeOD	0,13	-0,09	-0,06	-0,06	-0,08							
	CDCl3	0,15	-0,03	-0,02	-0,02	-0,02							
	Pyridin	0,21	0,03	0,05	0,03	0,04							
1-Aminoindan	MeOD	0,18	0,04	-0,01	-0,02	0,00	0,02	0,01	0,00	-0,03			
	CDCl3	0,15	0,02	-0,03	0,00	-0,01	-0,01	-0,02	-0,02	-0,01			
	Pyridin	0,18	0,08	-0,01	-0,02	0,00	0,00	0,00	-0,01	0,02			
Diethylamine	MeOD	0,06	0,00										
	CDCl3	0,19	0,07										
	Pyridin	0,10	0,03										
Cyclohexylamine	MeOD	0,18	0,06	0,01	0,02								
	CDCl3	0,22	0,10	0,01	0,03								
	Pyridin	0,18	0,07	-0,01	0,01								
2-(Methylamino)ethanol	MeOD	0,06	0,06	0,05									
	CDCl3	0,03	0,10	0,07									
	Pyridin	0,11	0,12	0,09									
2-(Methoxyethyl)methylamine	MeOD	0,04	-0,02	0,08	0,00								
	CDCl3	0,07	-0,01	0,09	0,01								
	Pyridin	0,10	0,01	0,10	0,00								

Figure 6-1 Various DIS values (in ppm) for chemicals with different functional groups and in three different solvents.

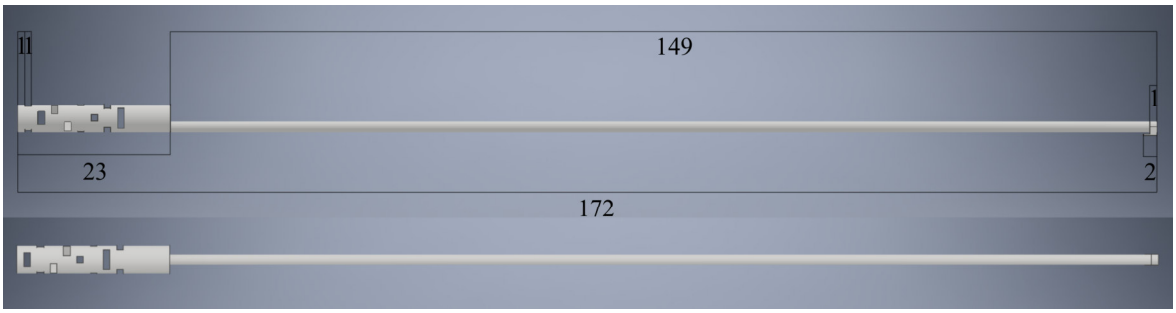

Figure 6-2 The exact dimensions of the first prototype from the x- and z-view. These dimensions were also taken for the second prototype, except for the size of the chamber.

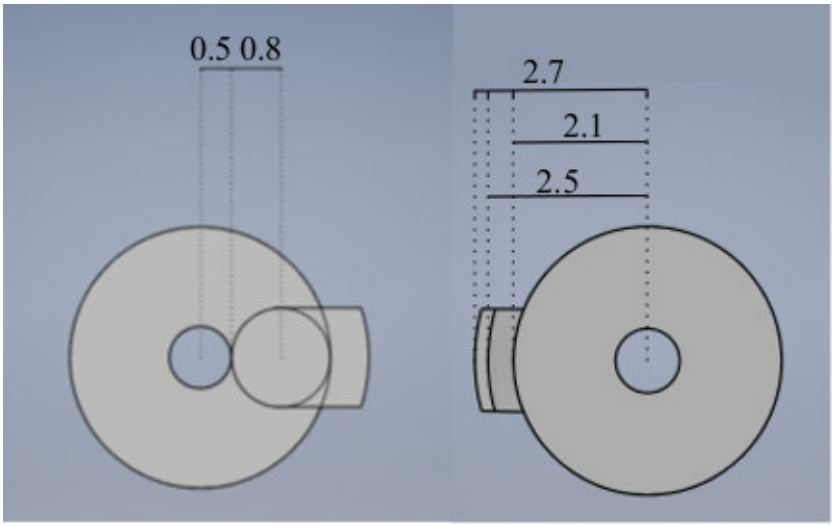

Figure 6-3 The exact dimensions of the first prototype from the y-views. These dimensions were also taken for the second prototype.

6.1. Curriculum Vitae

Personal Data

Name:	Martin Walenta, BSc
Address:	Millöckergasse 22, 8010 Graz
Date and Place of Birth:	03.01.1994 in 8570 Voitsberg
Nationality:	Austria
Personal Status:	unmarried

Education

03/2018 - Today	Masterthesis: *Improving NMR measurements by utilizing deuterium isotopic effects, inlays and cyclodextrins* at Prof. Klaus Zangger
10/2016 - Today	Masterstudies in Chemistry (NaWi-Studies at TU Graz and Karl Franzens University)
07/2016	Internship (Institute for Analytical Chemistry at Karl Franzens University) at Prof. Walter Gössler
10/2013 - 08/2016	Bachelorstudies in Chemistry (NaWi-Studies at TU Graz and Karl Franzens University) Bachelor Thesis: *Aminotroponiminat-Derivat als molekularer Schalter* at Prof. Leonhard Grill
10/2012 - 06/2013	Civilian Service
09/2004 - 06/2012	Academic High School (BG/BRG Carneri, Graz)
09/2000 - 07/2004	Elementary School (Volksschule Geidorf, Graz)